JOURNAL OF CHEMICAL INFORMATION AND MODELING

Letter

pubs.acs.org/jcim

Use of 3D Properties to Characterize Beyond Rule-of-5 Property Space for Passive Permeation

Cristiano R. W. Guimarães,* Alan M. Mathiowetz, Marina Shalaeva, Gilles Goetz, and Spiros Liras

Worldwide Medicinal Chemistry Department, Pfizer Global Research and Development, Eastern Point Road, Groton, Connecticut 06340, United States

Supporting Information

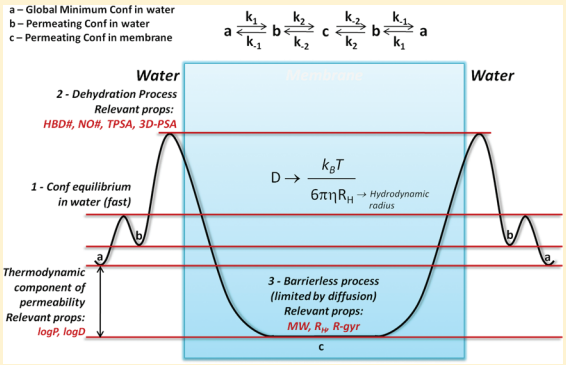

ABSTRACT: The application of conformationally dependent measures of size and polarity to characterize beyond rule-of-5 (Ro5) space for passive permeation was investigated. Specifically, radius of gyration, an alternative to molecular weight, and three-dimensional polar surface area and the generalized Born/surface area dehydration free energy, alternatives to hydrogen-bond donor and acceptor counts, were computed on models of the permeating conformations of over 35 000 molecules. The resulting guidelines for size and polarity, described by the 3D properties, should aid the design of Ro5 violators with passive permeability.

In the 1890s, Ernst Overton discovered that substances that dissolve in lipids pass more easily into a cell than those that dissolve in water. This was some of the first evidence that cells were surrounded by a lipid membrane. The correlation between permeability and solubility in lipids has since been called Overton's Rule.[1] More recently, a more complex view emerged where passive permeability across membranes was determined by solubility of the permeating molecule in the membrane, the diffusion across the membrane into the cell, and the thickness of the barrier.[2]

If this view is elaborated further, the permeation of molecules across the cell membrane becomes a function of three fundamental molecular properties: polarity, size, and lipophilicty, which ultimately dictate the free-energy profile illustrated in Figure 1. Specifically, the first step consists of an equilibrium between (a) the global minimum conformation and (b) the permeating conformation (or ensembles thereof) in water. Assuming this equilibrium is fast and that the energy gap between (a) and (b) is not significant, this step becomes unimportant to the kinetics of permeation. The barrier to enter the cell is then reasonably approximated by the free-energy cost associated with the desolvation of polar groups upon insertion in the membrane. Once inside the membrane, the molecule diffuses through a barrierless process according to the Stokes–Einstein equation,[3] where D, k_B, T, η, and R_H are the diffusion coefficient, Boltzmann constant, temperature, medium viscosity, and the hydrodynamic radius, respectively. R_H is defined as the radius of the equivalent hard sphere that diffuses at the same rate as the molecule; the behavior of this sphere includes hydration and shape effects. Finally, the free energy difference between the states where the molecule is inside the membrane (c) and in water (a), a measure of its lipophilicity, is the thermodynamic component of the permeation process. If a molecule is too hydrophilic, its partition is not thermodynamically favorable. On the other hand, if it is too lipophilic, the barrier to exit the membrane becomes relevant and affects the kinetics of permeation.

$$D = \frac{k_B T}{6\pi\eta R_H} \quad (1)$$

In 1997, Lipinski and co-workers described a set of rules for drug-likeness called the rule of 5 (Ro5). The rules define specific limits for molecular weight (MW), counts of hydrogen-bond donors and acceptors (HBD# and NO#), and the calculated partition coefficient between water and octanol (ClogP) that were important for the pharmacokinetics of drugs in the body, including absorption, distribution, metabolism, and excretion.[4] In the case of passive permeation, and consequently absorption, MW is used as an alternative to R_H to assess the impact of size on the diffusion of molecules across the cell membrane. HBD# and NO# describe the dehydration of polar groups from water to the membrane. The polarity of a molecule is often represented by the topological PSA (TPSA) since it is a fast method due to its conformational independence.[5] Finally, ClogP is used to assess the impact of lipophilicity in the partition of the molecule between the two environments.

This work was motivated by the observation that while Ro5 compliant molecules have good passive permeability, so do many Ro5 violators, including oral drugs (see below). This might have its origin in the suitability of the MW and HBD#/NO# descriptors as measures of size and polarity, respectively, in particular as molecules become larger and more complex. For example, a more extended molecule will have a larger R_H, and consequently lower D, than a more compact molecule of

Published: March 6, 2012

   dx.doi.org/10.1021/ci300010y | J. Chem. Inf. Model. 2012, 52, 882–890

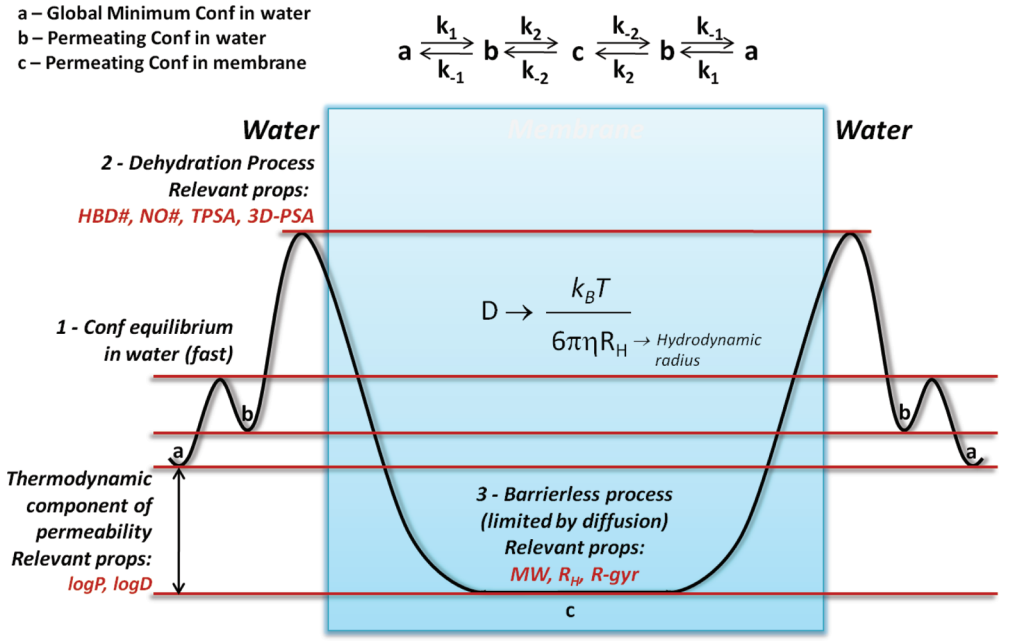

Figure 1. The permeation process in details and the key properties that govern the free-energy profile.

the same MW. In the case of HBD#/NO#, their conformational independence overestimates polarity for molecules that are able to hide it through the formation of intramolecular hydrogen bonds (HBs) or some other intramolecular interaction established in the permeating conformation.

Understanding what makes Ro5 violators have good passive permeability is extremely important since an increasing number of pharmaceutically relevant targets bind preferentially compounds that fall beyond Ro5 space, like those involved in the disruption of protein−protein interactions, peptidic G-protein-coupled receptors, and proteases.[6] As a matter of fact, a recent analysis demonstrated that newly launched drugs are shifting away from the traditional drug space. On average, they are larger molecules but not necessarily more lipophilic than older drugs.[7] In this work, we investigate the application of conformationally dependent measures of size and polarity to characterize beyond Ro5 space for passive permeation. Specifically, radius of gyration (R-gyr)[8] was chosen as an alternative property to MW. R-gyr is used instead of R_H because while the former can be calculated as the root-mean-square distance between the molecule's atoms and its center of gravity, the latter is experimentally derived from size exclusion chromatography or dynamic light scattering. R-gyr and R_H are numerically similar.[9] In the case of polarity, the three-dimensional polar surface area (3D-PSA)[10] and the dehydration free energy (ΔG_{dehyd}) estimated by the generalized Born/surface area (GB/SA) continuum model[11] were explored as alternatives to HBD#/NO# and TPSA. No 3D alternative for molecular lipophilicity was sought as the performance of such methods is poor when compared to substructure-based (atom or fragment) methods.[12] As the fragment-based approach in the ClogP method is fitted to reproduce experimental values, it should somewhat capture conformational effects in the partition process.[13] However, one should keep in mind that the fragment-based approach might fail for molecules that are much larger and bear increased conformational complexity than the training set used to derive the ClogP fragment contributions. As a matter of fact, as shown in ref 12, the performance of any logP method gradually decreases as the number of heavy atoms increases beyond 17−18.

To understand the impact of 3D molecular properties on passive permeation, a total of 35 170 compounds with passive permeability (P_{app}) data have been selected from our corporate database. The absence of unknown stereogenic centers and ionizable groups dictated the data set selection. In the former, this was necessary because the analysis involves the calculation of the 3D properties R-gyr, 3D-PSA, and ΔG_{dehyd}, whereas in the latter, it was done to eliminate the negative impact of charged species on passive permeability. Assuming neutralization is required for permeation, the presence of ionizable groups would: (a) add an energy penalty associated with the neutralization of the molecule followed by its desolvation upon insertion in the membrane and (b) impact the thermodynamics of the permeation process by reducing the molecule's lipophilicty, both a function of the difference between the molecule's pK_a and the medium pH. In the absence of measured pK_a's, it is safer to focus only on nonionizable compounds in order to simplify the analysis.

Conformational analysis was performed in chloroform, and the lowest energy conformation of each compound, assumed to be a good representation of the permeating conformation, was used to obtain the 3D properties. Previous computational studies used chloroform to represent the membrane environment[14] since it is a nonhydrogen-bonding solvent with a dielectric constant similar to that calculated for the center of a lipid bilayer.[15]

The Data Set. Figure 2 illustrates the distribution of Ro5 properties for the data set selected. It is clear that just a small portion of the data set displays violations of MW, HBD#, NO#, and ClogP, reflecting Ro5 compliance by our medicinal chemists. Although this is an unbalanced data set, heavily populated by Ro5 compliant small molecules, we can still learn from the subset containing Ro5 violators. For example, Figure 2 illustrates that passive permeability becomes progressively poorer as the number of Ro5 violations increases. However, a significant number of them still displays moderate to high

dx.doi.org/10.1021/ci300010y | J. Chem. Inf. Model. 2012, 52, 882−890

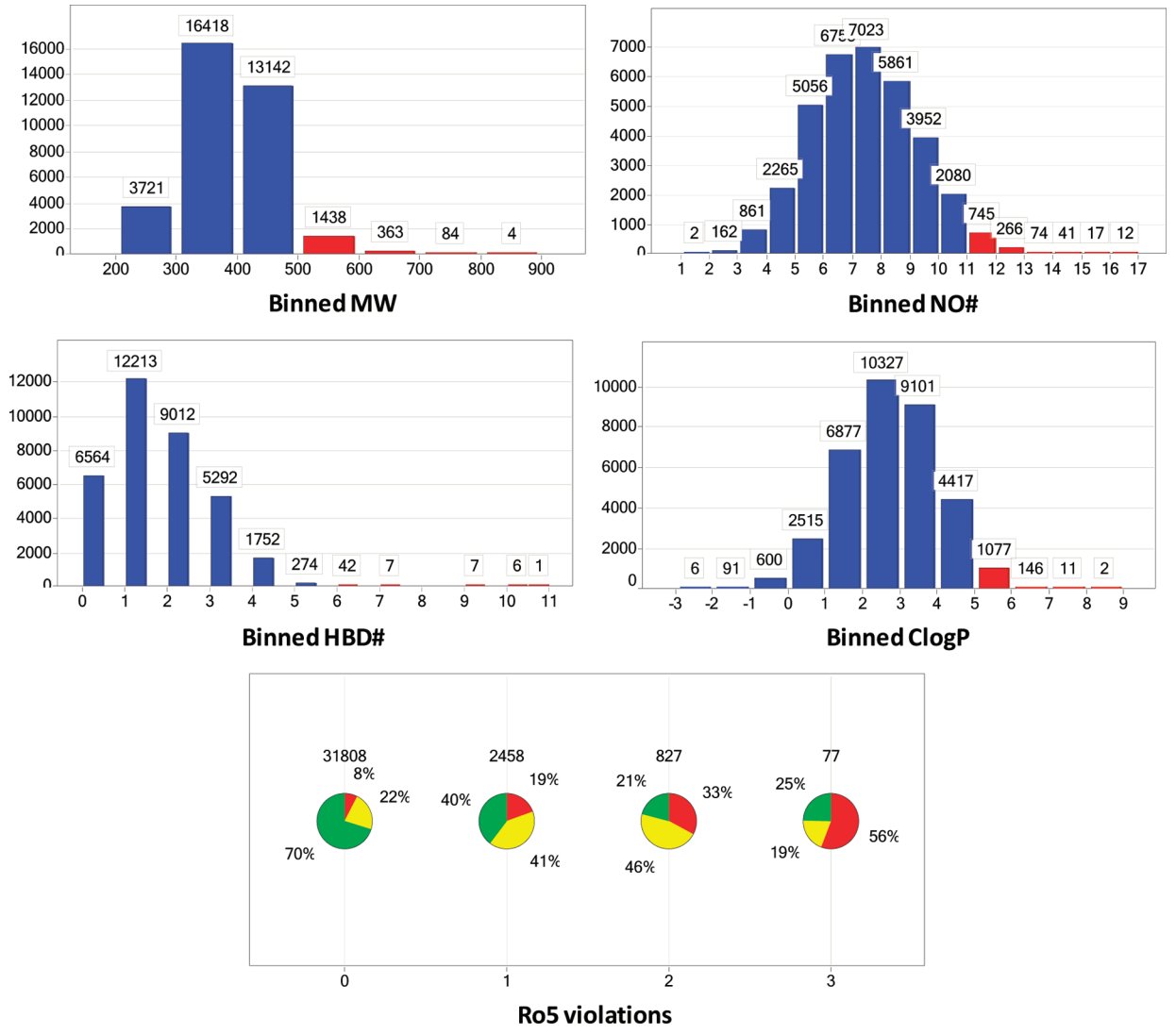

Figure 2. Lipinski's Ro5 property distributions. Violations of MW, NO#, HBD#, and ClogP are shown in red. Also shown is the impact of Ro5 violations on passive permeability (bottom). High, moderate, and low permeabilities are colored green, yellow, and red, respectively. See text for P_{app} ranges.

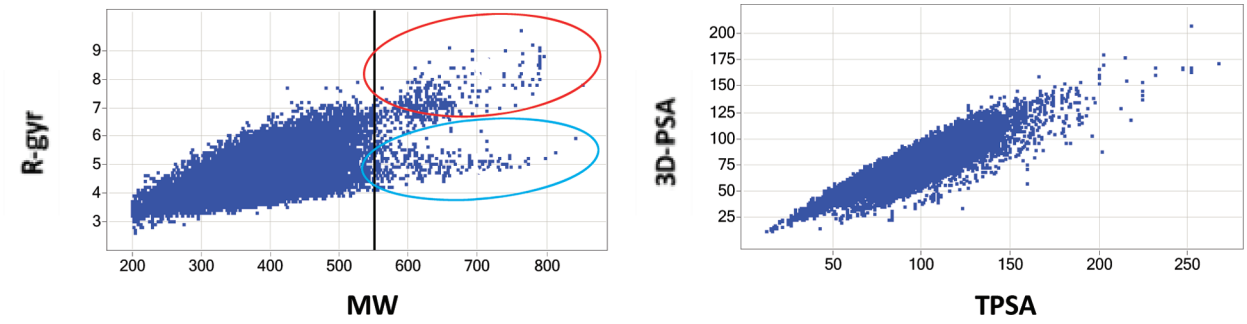

Figure 3. Plots of MW versus R-gyr (left) and TPSA versus 3D-PSA (right).

passive permeability; the specific limits for high, moderate, and poor passive permeability behavior, as characterized by the experiment, are $P_{app} \geq 10 \times 10^{-6}$ cm/s, 2.5×10^{-6} cm/s $\leq P_{app} < 10 \times 10^{-6}$ cm/s, $P_{app} < 2.5 \times 10^{-6}$ cm/s, respectively. Despite MW, HBD#, and NO# violations, it is likely that the size and polarity of such molecules translate into moderate to high passive permeability by means of specific permeating conformations that behave like Ro5 compliant small molecules.

Size. The impact of size as described by R-gyr on passive permeability and its relationship with MW were analyzed. A plot of MW versus R-gyr shows that the latter gets scattered at larger MW values (Figure 3). This should be expected since the conformational space becomes more complex as MW increases. In other words, a greater variety of R-gyr values is obtained per MW. In the data set studied, 33 281 molecules out of 35 170 have MW $\leq$ 500. Almost all of the low-MW subset, except for

dx.doi.org/10.1021/ci300010y | J. Chem. Inf. Model. 2012, 52, 882−890

16 molecules, have R-gyr ≤ 7 Å, suggesting this value as a reasonable limit to differentiate between small- and large-sized molecules. It also suggests that size does not play a significant role on the permeability distribution for the data set studied, since merely 249 molecules have R-gyr above the cutoff. However, the importance of size to passive permeability must not be downplayed. One way to evaluate the relevance of R-gyr is to analyze its impact on the P_{app} values of molecules with very high MW. Figure 3 shows that the region between MW values of 500 and 550 is heavily populated with compounds (over 1000 compounds), indicating that excursions to borderline MW violations are frequent. Most of the compounds in this MW range also display R-gyr ≤ 7 Å. At MW > 550, however, the distribution becomes sparse and diverges in two clusters, one displaying lower R-gyr values (blue circle) and the other one higher R-gyr values (red circle) than the cutoff. Figure 4

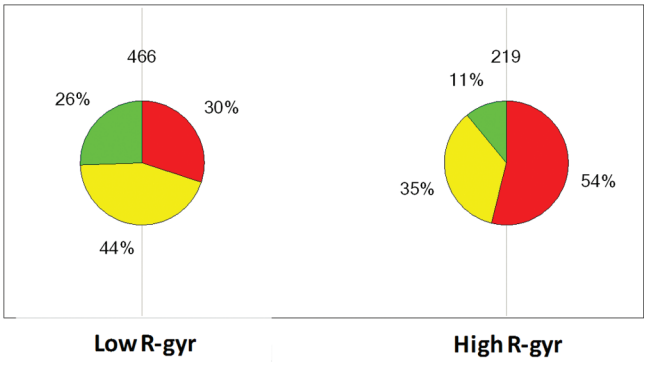

Figure 4. Impact of R-gyr on P_{app} for the subset with MW > 550. High, moderate, and low permeabilities are colored green, yellow, and red, respectively. The R-gyr cutoff is 7 Å. See text for P_{app} ranges.

shows that the compounds from the MW > 550 group with R-gyr values above 7 Å tend to have much poorer P_{app} values. To eliminate the contributions of other properties that govern permeability, the same plot was generated for a subset with optimal polarity and lipophilicity ranges, as defined below, and similar P_{app} distributions emerged for the low and high R-gyr subsets.

Polarity and Lipophilicty. In Figure 3, it is clear that the TPSA values are in general much higher than the 3D-PSA values of the conformations generated in chloroform. Although the TPSA atomic parameters were developed to reproduce 3D-PSA values, the conformations used in the fitting process in the work of Ertl et al.[5] were not a result of a conformational analysis performed in a hydrophobic environment but rather generated by CORINA;[10] intramolecular hydrogen bonds are likely not present in the CORINA conformations. Hence, TPSA overestimates the polarity of permeating conformations. While the two measures might provide similar values for relatively small, rigid molecules, that should not be the case for large, flexible, likely non-Ro5 compliant molecules, capable of establishing intramolecular interactions that hide polarity when in a hydrophobic environment.

Figure 5 shows the impact of polarity, as described by 3D-PSA or alternatively ΔG_{dehyd}, and lipophilicity, as described by ClogP, on passive permeability. The combinations of 3D-PSA and ClogP or ΔG_{dehyd} and ClogP are more discriminating than when those properties are analyzed separately. The optimal 3D-PSA value to characterize high and low polarity for the data set studied was 100 Å^2, which roughly corresponds to a value of +23.5 kcal/mol for ΔG_{dehyd}. These cutoffs are the ones that better enrich the low polarity subset with high P_{app} values and the high polarity subset with low P_{app} values, with similar results for 3D-PSA and ΔG_{dehyd} in terms of the molecule count in each sector as well as their respective distributions. The smaller cutoff obtained for 3D-PSA in contrast to the work of Clark[10] (140 Å^2) is likely due to the different approaches used to generate the conformations as discussed above. In spite of its conformational independence, we observed that a TPSA cutoff of 125 Å^2 is as discriminatory as 3D-PSA and ΔG_{dehyd}, suggesting that the conformational search step is not advantageous, at least for the full data set, heavily populated with low-MW molecules (see Supporting Information).

As for lipophilicty, the ideal ClogP range for permeability is between 0 and 3, followed by the more lipophilic range between 3 to 5. The extremes for lipophilicity, when ClogP is less than 0 or greater than 5, tend to display P_{app} distributions that contain molecules with poorer permeabilities than the other subsets. This is easily understood with the aid of Figure 1. The permeability process for molecules that are too hydrophilic is thermodynamically unfavorable. In the case of very hydrophobic molecules, their highly favorable solvation in the membrane environment slows down their permeation; the barrier to exit the membrane becomes too high. A sweet spot for passive permeability then emerges when the optimal ClogP and 3D-PSA or ΔG_{dehyd} ranges are combined. This sector contains molecules with distributions of high, moderate, and low P_{app} values of 77, 17, and 6% when 3D-PSA (or TPSA) and 80, 15, and 5% when ΔG_{dehyd} are used as measures of polarity. In all cases, the sweet spot for passive permeability is enriched with high-permeability molecules when compared to the corresponding distribution for the full data set, 67, 24, and 9%.

Beyond Ro5 space. To examine the utility of these guidelines in the characterization of passive permeability beyond Ro5 space, a subset containing molecules with at least two Ro5 violations, one of them being MW, was selected from the full data set. One should keep in mind that Lipinski's Ro5 guidelines allow one violation.[4] This subset contains 892 molecules. Figure 6 shows how the combinations of 3D-PSA and ClogP or ΔG_{dehyd} and ClogP perform for the subset with two Ro5 violations. In this case, the performance of TPSA is somewhat inferior when compared to 3D-PSA (see Supporting Information). For instance, the sweet spot for passive permeability defined by ClogP and 3D-PSA displays a distribution of high, moderate, and low P_{app} values of 33, 56, and 11%, which compares to 29, 54, and 17% in the case of ClogP and TPSA. The ability to establish intramolecular hydrogen bonds or other intramolecular interactions that hide polarity in a hydrophobic environment increases as molecules become larger and more flexible, hence the conformational search step might become essential to accurately describe the molecular polarity upon permeation. ΔG_{dehyd} seems to perform even better for the optimal ClogP range, with a distribution of high, moderate, and low P_{app} values of 48, 41, and 11%. The sweet spot for passive permeability in each case contrast with the distribution for the full beyond Ro5 subset, 21, 44, 35%; a clear enrichment is obtained, in particular with ΔG_{dehyd}.

It is plausible that the difference between the results using 3D-PSA (or TPSA) and ΔG_{dehyd} for large molecules has its origin in the assumption when PSA is used as an estimate of polarity that all hydrogen bonds between atoms of the same type and water are equivalent. While this is reasonable when molecules are small, one can easily understand that this would

dx.doi.org/10.1021/ci300010y | J. Chem. Inf. Model. 2012, 52, 882−890

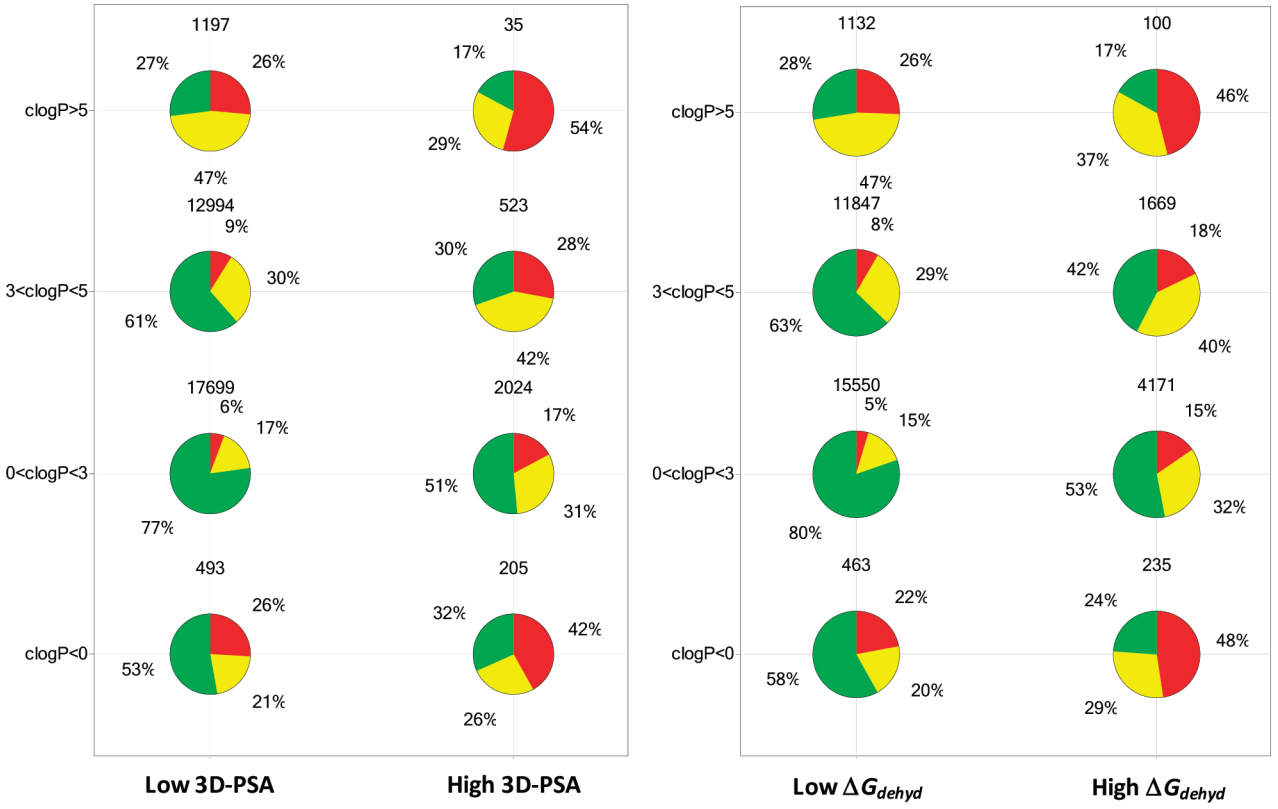

Figure 5. Impact of lipophilicity (ClogP) and polarity, as described by 3D-PSA (left) and ΔG_{dehyd} (right), on P_{app} for the full data set. High, moderate, and low permeabilities are colored green, yellow, and red, respectively. The 3D-PSA and ΔG_{dehyd} cutoffs are 100 Å^2 and +23.5 kcal/mol, respectively. See text for P_{app} ranges.

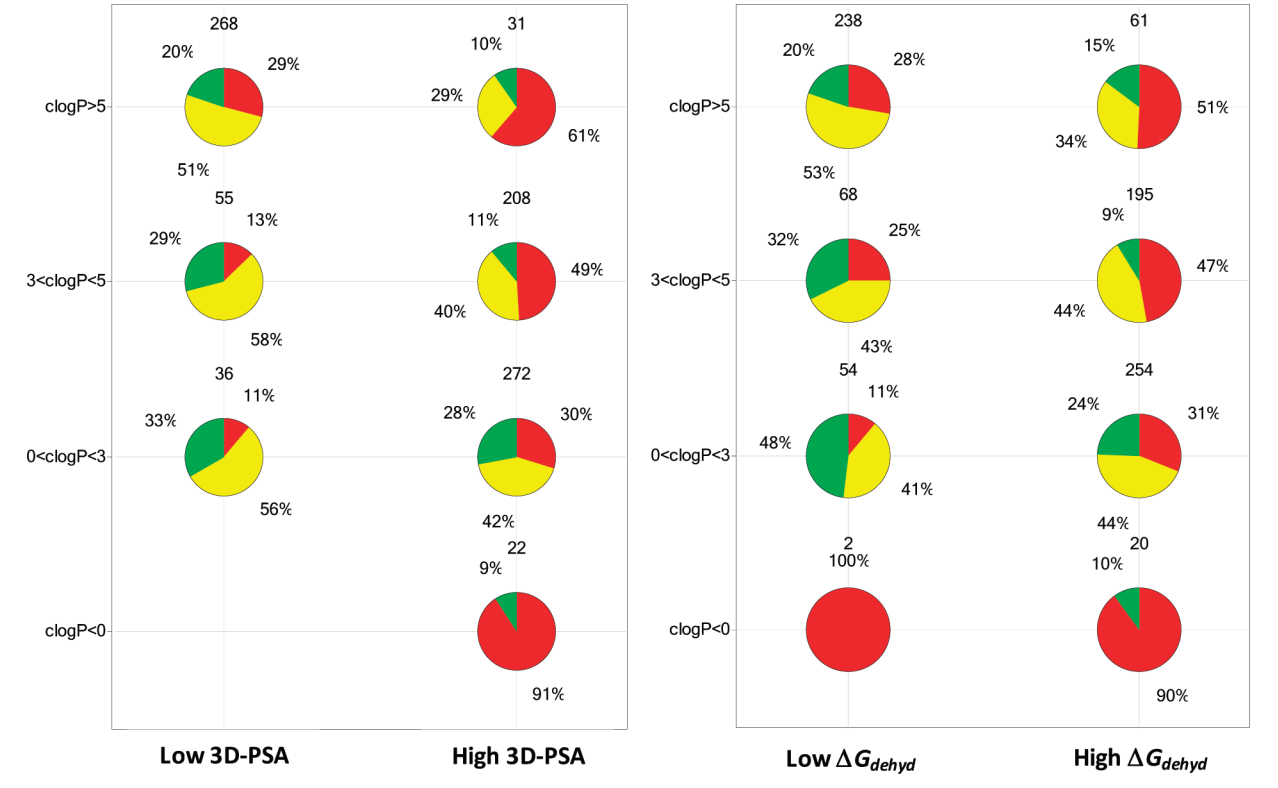

Figure 6. Impact of lipophilicity (ClogP) and polarity, as described by 3D-PSA (left) and ΔG_{dehyd} (right), on P_{app} for beyond Ro5 subset. High, moderate, and low permeabilities are colored green, yellow, and red, respectively. The 3D-PSA and ΔG_{dehyd} cutoffs are 100 Å^2 and +23.5 kcal/mol, respectively. See text for P_{app} ranges.

dx.doi.org/10.1021/ci300010y | J. Chem. Inf. Model. 2012, 52, 882−890

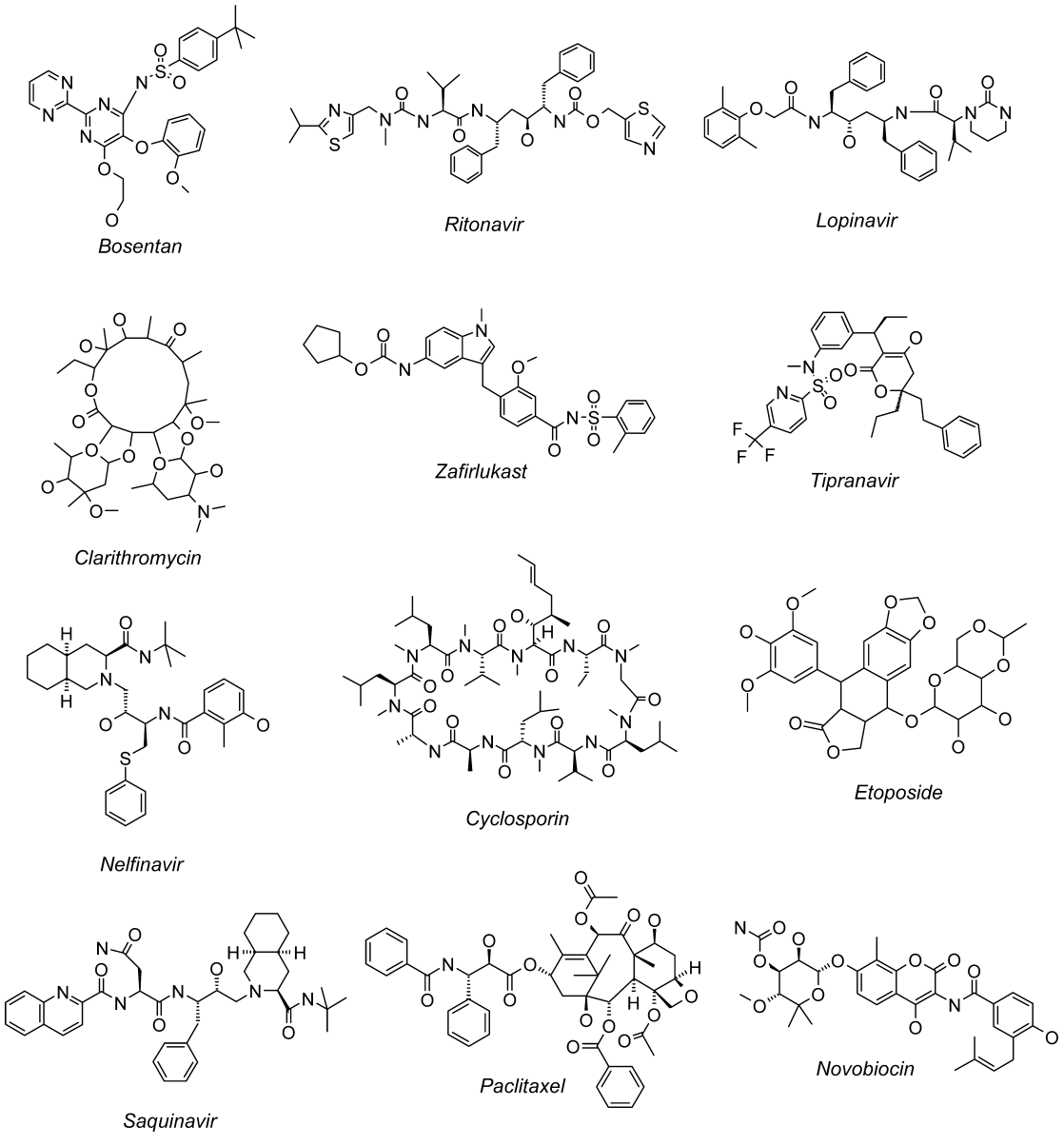

Figure 7. Beyond Ro5 oral drugs with at least two Ro5 violations. They all violate the MW cutoff.

Table 1. Experimental LogD, Ro5, and 3D Properties and Measured P_{app} for Beyond Ro5 Oral Drugs

	MW	ClogP	HBD#	NO#	TPSA	R-gyr	logD[a]	3D-PSA	ΔG_{dehyd}	ion.[b]	P_{app}[c] × 10^6
bosentan	*552*	4.2	2	*11*	*154*	4.5	1.2	98	18.6	yes	10.8
ritonavir	*721*	4.9	4	*11*	*202*	4.9	*4.90*	89	19.7	no	2.75
lopinavir	*629*	*6.1*	4	9	120	4.7	*5.40*	66	12.2	no	4.35
clarithromycin	*748*	2.4	4	*14*	*183*	5.3	1.5	*121*	17.7	yes	8.33
zafirlukast	*576*	*7.1*	2	9	124	6.6	2.8	*101*	15.6	yes	3.70
tipranavir	*617*	*6.9*	1	7	105	6.1	*7.4*	80	12.7	yes	6.77
nelfinavir	*568*	*5.8*	4	7	*127*	5.6	*6.1*	80	16.5	yes	1.39
cyclosporin	*1203*	*14.4*	5	*23*	*279*	6.6	*8.5*	*144*	*25.4*	no	1.07
etoposide	*589*	0.0	3	*13*	*161*	5.4	0.9	*158*	*30.7*	no	0.81
saquinavir	*671*	4.7	*6*	*11*	*167*	6.4	*5.9*	*126*	19.0	yes	1.36
paclitaxel	*854*	4.7	4	*15*	*221*	5.8	*3.4*	*183*	*24.6*	no	1.16
novobiocin	*613*	4.0	*6*	*13*	*200*	*7.7*	1.4	*159*	*23.9*	yes	1.18
cutoffs	500	5.0	5	10	125 Å^2	7.0 Å	3.0	100 Å^2	23.5	–	

[a]Shake−Flask and HPLC logD's were obtained for each molecule. Shake−Flask logD values are only reliable up to 3.5. Above that value, the HPLC logD value was used in the analysis. [b]Ionizable. [c]$P_{app} \geq 10 \times 10^{-6}$ cm/s (high permeability), 2.5×10^{-6} cm/s $\leq P_{app} < 10 \times 10^{-6}$ cm/s (moderate permeability), $P_{app} < 2.5 \times 10^{-6}$ cm/s (low permeability).

dx.doi.org/10.1021/ci300010y | J. Chem. Inf. Model. 2012, 52, 882−890

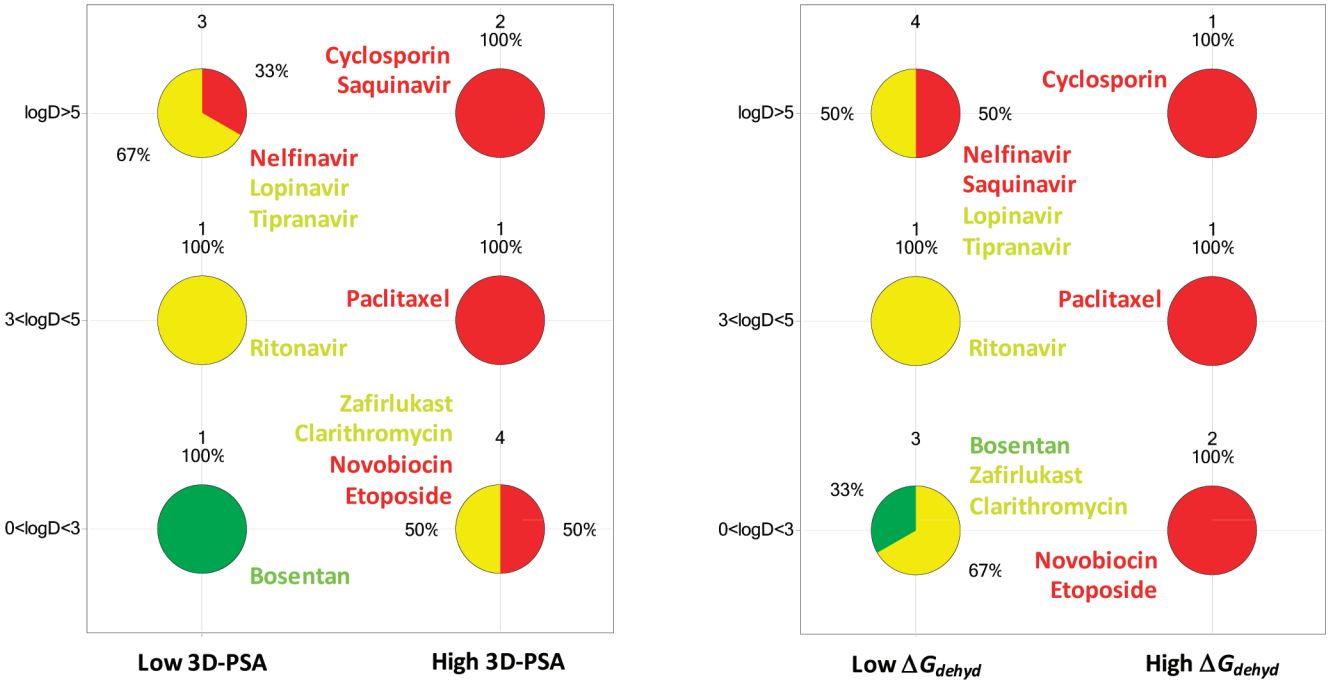

Figure 8. Impact of lipophilicity (experimental logD) and polarity, as described by 3D-PSA (left) and ΔG_{dehyd} (right), on P_{app} for beyond Ro5 oral drugs. High, moderate, and low permeabilities are colored green, yellow, and red. The 3D-PSA and ΔG_{dehyd} cutoffs are 100 Å^2 and +23.5 kcal/mol, respectively. See text for P_{app} ranges.

fail as molecules increase in size and number of polar atoms; the electron-withdrawing effects of all nitrogens and oxygens in a molecule should overall weaken their hydrogen bonds to water. These effects should be captured by ΔG_{dehyd}, as it uses partial charges derived from quantum mechanical calculations.[16] Figure 6 shows that a net of 18 molecules moves from the high to the low polarity group for the ClogP subset between 0 and 3 when ΔG_{dehyd} is used instead of 3D-PSA. For the more hydrophobic subset, between 3 and 5, this occurs for a net of 13 molecules. The more hydrophobic subsets contain molecules with fewer polar atoms and, consequently, less pronounced electron-withdrawing effects. In this manner, a reverse migration between the high and low polarity groups arises for the subset with ClogP > 5. The Supporting Information contains the migration patterns between populations when polarity defined by 3D-PSA is replaced by ΔG_{dehyd} for the full and the beyond Ro5 sets.

In order to further test the guidelines, 12 oral drugs containing at least two Ro5 violations, one of them being MW, were selected. In this case, the selection was extended to ionizable molecules as well since the majority of the oral drugs with two Ro5 violations in our corporate collection has either a basic or acidic center (Figure 7). To include the impact of charge on lipophilicity, experimental logD's were obtained using both the Shake−Flask and HPLC methods. The HPLC logD was used as a measure of lipophilicity whenever the Shake−Flask logD was above 3.5; the latter is not reliable above that value. Table 1 lists the experimental logD value used as well as the Ro5 properties, TPSA, the 3D properties R-gyr, 3D-PSA, and ΔG_{dehyd}, and the measured P_{app} values. It should be noted that the 3D properties were obtained from conformational analysis of the ionizable molecules in their neutral state, likely to be the state adopted upon permeation. The Ro5, TPSA, and the 3D property violations are underlined in Table 1. Except for bosentan, all molecules have either poor or moderate passive permeability. As most of them have reasonable bioavailabilities,[17−28] it would not be surprising if active transport mechanisms were involved in their incorporation into the body. A comparison between a low passive permeability P_{app} value of 1.07×10^{-6} cm/s and a Caco-2 P_{app} value of 6.00×10^{-6} cm/s (data generated in-house), considered high for the Caco-2 cell line, suggests that this is the case for cyclosporin.

In the absence of measured pK_a's, it is impossible to quantify the contribution of the neutralization penalty on the barrier to enter the cell for the ionizable molecules. However, this can be indirectly assessed through the comparison of the calculated ClogP for the neutral species and the experimental logD values. Table 1 shows that both agree within one log unit for almost all molecules, except for the ionizable Bosentan, Zafirlukast, and Novobiocin, and the nonionizable Cyclosporin. In the latter, this is likely associated with failure by the ClogP fragment-based approach to estimate the lipophilicty for a molecule that is much larger than the training set. The much lower experimental logD values for bosentan, zafirlukast, and novobiocin when compared to ClogP suggest they are highly ionized at physiological pH. In other words, the neutralization penalty before the desolvation step might play an important role in their passive permeabilities. Therefore, it is plausible that TPSA, 3D-PSA, and ΔG_{dehyd} do not provide a good approximation for the barrier to enter the membrane in those cases. Figure 8 illustrates that the combination of polarity, using either 3D-PSA or ΔG_{dehyd}, and lipophilicity, using the experimental logD values, is highly predictive of passive permeability behavior, regardless of the ionization state and Ro5 violations. Again, 3D-PSA seems to overestimate polarity when compared to ΔG_{dehyd}; zafirlukast, clarithromycin, and saquinavir move from the high to the low polarity group when ΔG_{dehyd} is used as a measure of polarity. This data set is particularly problematic for the conformationally independent

dx.doi.org/10.1021/ci300010y | J. Chem. Inf. Model. 2012, 52, 882−890

TPSA as the polarity of all molecules, except tipranavir, lopinavir, and zafirlukast, is classified as high, the last two being borderline low polarity (Table 1). In addition, bosentan, the only molecule with high passive permeability, has a TPSA value of 154 Å^2, significantly above the cutoff of 125 Å^2. Finally, all molecules in Table 1, except for novobiocin, have R-gyr below 7 Å, suggesting that the passive permeabilities for this subset should not be adversely impacted by size. In summary, the guidelines provided by the conformationally dependent measures of size (R-gyr) and polarity (3D-PSA and ΔG_{dehyd}) as well as lipophilicity, described by ClogP or experimental logD, seem to aid the design of Ro5 violators with passive permeability. Molecules that fall in the space where R-gyr $\leq$ 7 Å, 3D-PSA $\leq$ 100 Å^2 or ΔG_{dehyd} < +23.5 kcal/mol, and 0 $\leq$ ClogP < 3 are more likely to permeate passively regardless of large MW and HBD/NO counts. The alternative properties and their ranges could be used as filters in HTS triaging and virtual screening.

Experimental Procedures. The MCMM method implemented in MacroModel[29] was used to perform the conformational analysis in chloroform using the OPLS_2005 force field[16] to describe the solute and the GB/SA method[11] to describe the solvent. The default settings were used for molecules with MW up to 500 and increased by 10-fold for high MW molecules. R-gyr and 3D-PSA estimates were generated using the global minimum conformation obtained in chloroform for each molecule. This conformation was also used to generate ΔG_{dehyd}, taken as the negative of the GB/SA hydration energy, obtained via a single-point energy calculation in water. TPSA was obtained as described in ref 5. LogP was predicted using Biobyte software.[30]

Passive permeability data were obtained at pH 7.4 using the MDCKII-LE cell line. The cells were generated in-house as a subclone of MDCK wild-type cells displaying low expression of active transporters. For details, see ref 31. Experimental logD values were obtained at pH 7.4 using both the Shake−Flask[32] and HPLC methods.[33]

■ ASSOCIATED CONTENT

Supporting Information

The impact of ClogP and TPSA on P_{app} and the migration patterns between populations when polarity defined by 3D-PSA is replaced by ΔG_{dehyd} for the full and the beyond Ro5 sets (Figures 5 and 6). This material is available free of charge via the Internet at http://pubs.acs.org.

■ AUTHOR INFORMATION

Corresponding Author

*E-mail: cristiano.guimaraes@pfizer.com. Telephone: (860) 686-2915.

Notes

The authors declare no competing financial interest.

■ REFERENCES

(1) Al-Awqati, Q. One hundred years of membrane permeability:-Does Overton still rule? *Nat. Cell Biol.* **1999**, *1*, E201−E202.
(2) Lieb, W. R.; Stein, W. D. The molecular basis of simple diffusion within biological membranes. *Curr. Top. Membr. Transp.* **1971**, *2*, 1−39.
(3) Kholodenko, A. L.; Douglas, J. F. Generalized Stokes-Einstein equation for spherical particle suspensions. *Phys. Rev.* **1995**, *E 51/2*, 1081−1090.
(4) Lipinski, C. A.; Lombardo, F.; Dominy, B. W.; Feeney, P. J. Experimental and computational approaches to estimate solubility and permeability in drug discovery and development settings. *Adv. Drug Delivery Rev.* **1997**, *23*, 3−25.
(5) Ertl, P.; Rohde, B.; Selzer, P. Fast calculation of molecular polar surface area as a sum of fragment-based contributions and its application to the prediction of drug transport properties. *J. Med. Chem.* **2000**, *43*, 3714−3717.
(6) Alex, A.; Millan, D. S.; Perez, M.; Wakenhut, F.; Whitlock, G. A. Intramolecular hydrogen bonding to improve membrane permeability and absorption in beyond rule of five chemical space. *Med. Chem. Commun.* **2011**, *2*, 669−674.
(7) Faller, B.; Ottaviani, G.; Ertl, P.; Berellini, G.; Collis, A. Evolution of the physicochemical properties of marketed drugs: can historyforetell the future? *Drug Discovery Today* **2011**, *16*, 976−984.
(8) Narang, P.; Bhushan, K.; Bose, S.; Jayaram, B. A computational pathway for bracketing native-like structures for small alpha helical globular proteins. *Phys. Chem. Chem. Phys.* **2005**, *7*, 2364−2375.
(9) Kok, C. M.; Rudin, A. Relationship between the hydrodynamic radius and the radius of gyration of a polymer in solution. *Makromol. Chem., Rapid Commun.* **1981**, *2*, 655−659.
(10) Clark, D. E. Rapid calculation of polar molecular surface area and its application to the prediction of transport phenomena. 1. Prediction of intestinal absorption. *J. Pharm. Sci.* **1999**, *88*, 807−814.
(11) Still, W. C.; Tempczyk, A.; Hawley, R. C.; Hendrickson, T. Semianalytical treatment of solvation for molecular mechanics and dynamics. *J. Am. Chem. Soc.* **1990**, *112*, 6127−6129.
(12) Mannhold, R.; Poda, G. I.; Ostermann, C.; Tetko, I. V. Calculation of molecular lipophilicity: State-of-the-art and comparison of Log P methods on more than 96,000 compounds. *J. Pharm. Sci.* **2009**, *98*, 861−893.
(13) Leo, A. J. Calculating log P_{oct} from structures. *Chem. Rev.* **1993**, *93*, 1281−1306.
(14) (a) Rezai, T.; Bock, J. E.; Vong, M.; Lokey, R. S.; Jacobson, M. P. Conformational flexibility, internal hydrogen bonding, and passive membrane permeability: Successful in silico prediction of the relative permeabilities of cyclic peptides. *J. Am. Chem. Soc.* **2006**, *128*, 14073−14080. (b) Swift, R. V.; Amaro, R. E. Modeling the pharmacodynamics of passive membrane permeability. *J. Comput.-Aided Mol. Des.* **2011**, *25*, 1007−1017.
(15) Koehorst, R. B.; Spruijt, R. B.; Vergeldt, F. J.; Hemminga, M. A. Lipid bilayer topology of the transmembrane alpha-helix of M13 major coat protein and bilayer polarity profile by site-directed fluorescence spectroscopy. *Biophys. J.* **2004**, *87*, 1445−1455.
(16) Kaminski, G. A.; Friesner, R. A.; Tirado-Rives, J.; Jorgensen, W. J. Evaluation and reparametrization of the OPLS-AA force field for proteins via comparison with accurate quantum chemical calculations on peptides. *J. Phys. Chem. B* **2001**, *105*, 6474−6487.
(17) Weber, C.; Gasser, R.; Hopfgartner, G. Absorption, excretion, and metabolism of the endothelin receptor antagonist Bosentan in healthy male subjects. *Drug Metab. Dispos.* **1999**, *27*, 810−815.
(18) Lledo-Garcia, R.; Nacher, A.; Prats-Garcia, L.; Casabo, V. G.; Merino-Sanjuan, M. Bioavailability and pharmacokinetic model for ritonavir in the rat. *J. Pharm. Sci.* **2007**, *96*, 633−643.
(19) Klein, C. E.; Chiu, Y.-L.; Cai, Y.; Beck, K.; King, K. R.; Causemaker, S. J.; Doan, T.; Esslinger, H.-U.; Podsadecki, T. J.; Hanna, G. J. Effects of acid-reducing agents on the pharmacokinetics of Lopinavir/Ritonavir and Ritonavir-boosted Atazanavir. *J. Clin. Pharmacol.* **2008**, *48*, 553−562.
(20) Garver, E.; Hugger, E. D.; Shearn, S. P.; Rao, A.; Dawson, P. A.; Davis, C. B.; Han, C. Involvement of Intestinal Uptake Transporters in the Absorption of Azithromycin and Clarithromycin in the Rat. *Drug Metab. Dispos.* **2008**, *36*, 2492−2498.
(21) Madhavi, B. R.; Devi, N. K. D.; Rani, A. P. Preparation and characterization of Zafirlukast-β-Cyclodextrin complexes using solid dispersion techniques. *Int. J. Pharm. Sci.* **2010**, *4*, 88−93.
(22) Temesgen, Z.; Feinberg, J. Tipranavir: A new option for the treatment of drug-resistant HIV infection. *Clin. Infect. Dis.* **2007**, *45*, 761−769.

(23) Kaldor, S. W.; Kalish, V. J.; Davies, J. F. II; Shetty, B. V.; Fritz, J. E.; Appelt, K.; Burgess, J. A.; Campanale, K. M.; Chirgadze, N. Y.; Clawson, D. K.; Dressman, B. A.; Hatch, S. D.; Khalil, D. A.; Kosa, M. B.; Lubbehusen, P. P.; Muesing, M. A.; Patick, A. K.; Reich, S. H.; Su, K. S.; Tatlock, J. H. Viracept (Nelfinavir Mesylate, AG1343): A potent, orally bioavailable inhibitor of HIV-1 protease. *J. Med. Chem.* **1997**, *40*, 3979−3985.

(24) Lindholm, A.; Kahan, B. D. Influence of cyclosporine pharmacokinetics, through concentrations, and AUC monitoring on outcome after kidney transplantation. *Clin. Pharmacol. Ther.* **1993**, *54*, 205−218.

(25) Hande, K. R.; Krozely, M. G.; Greco, F. A.; Hainsworth, J. D.; Johnson, D. H. Bioavailability of low-dose oral etoposide. *J. Clin. Oncol.* **1993**, *11*, 374−377.

(26) Winston, A.; Back, D.; Fletcher, C.; Robinson, L.; Unsworth, J.; Tolowinska, I.; Schutz, M.; Pozniak, A. L.; Gazzard, B.; Boffito, M. Effect of omeprazole on the pharmacokinetics of saquinavir-500 mg formulation with ritonavir in healthy male and female volunteers. *AIDS* **2006**, *20*, 1401−1406.

(27) Varma, M. V.S.; Panchagnula, R. Enhanced oral paclitaxel absorption with vitamin E-TPGS: Effect on solubility and permeability in vitro, in situ and in vivo. *Eur. J. Pharm. Sci.* **2005**, *25*, 445−453.

(28) Biganzoli, E. E.; Cavenaghi, L. A.; Rossi, R.; Brunati, M. C.; Nolli, M. L. Use of a Caco-2 cell culture model for the characterization of intestinal absorption of antibiotics. *Farmaco* **1999**, *54*, 594−599.

(29) *MacroModel*, version 9.0; Schrödinger, LLC: New York, 2005.

(30) *ClogP*; BioByte Corp.: Claremont, CA, 2000.

(31) Di, L.; Whitney-Pickett, C.; Umland, J. P.; Zhang, H.; Zhang, X.; Gebhard, D. F.; Lai, Y.; Federico, J. J. 3rd; Davidson, R. E.; Smith, R.; Reyner, E. L.; Lee, C.; Feng, B.; Rotter, C.; Varma, M. V.; Kempshall, S.; Fenner, K.; El-Kattan, A. F.; Liston, T. E.; Troutman, M. D. Development of a new permeability assay using low-efflux MDCKII cells. *J. Pharm. Sci.* **2011**, *100*, 4974−4985.

(32) Leo, A.; Hansch, C.; Elkins, D. Partition coefficients and their uses. *Chem. Rev.* **1971**, *71*, 525−616.

(33) Lombardo, F.; Shalaeva, M. Y.; Tupper, K. A.; Gao, F.. ElogDoct: A tool for lipophilicity determination in drug discovery. 2. Basic and neutral Compounds. *J. Med. Chem.* **2001**, *44*, 2490−2497.